energies

MDPI

Article

Effects of a Dual-Loop Exhaust Gas Recirculation System and Variable Nozzle Turbine Control on the Operating Parameters of an Automotive Diesel Engine

Giorgio Zamboni *, Simone Moggia and Massimo Capobianco

Internal Combustion Engines Group (ICEG), Department of Mechanical, Energy, Management and Transportation Engineering (DIME), University of Genoa, via Montallegro 1, 16145 Genoa, Italy; simone.moggia@edu.unige.it (S.M.); massimo.capobianco@unige.it (M.C.)

* Correspondence: giorgio.zamboni@unige.it; Tel.: +39-10-353-2457

Academic Editor: George Kosmadakis

Received: 23 September 2016; Accepted: 21 December 2016; Published: 4 January 2017

Abstract: Reduction of NO_X emissions and fuel consumption are the main topics in engine development, forcing the adoption of complex techniques and components, whose interactions have to be clearly understood for proper and reliable operations and management of the whole system. The investigation presented in this paper aimed at the development of integrated control strategies of turbocharging, high pressure (HP) and low pressure (LP) exhaust gas recirculation (EGR) systems for better NO_X emissions and fuel consumption, while analyzing their reciprocal influence and the resulting variations of engine quantities. The study was based on an extended experimental program in three part load engine operating conditions. In the paper a comparison of the behavior of the main engine sub-systems (intake and exhaust circuits, turbocharger turbine and compressor, HP and LP EGR loops) in a wide range of operating modes is presented and discussed, considering open and closed loop approaches for variable nozzle turbine (VNT) control, and showing how these affect engine performance and emissions. The potential of significant decrease in NO_X emissions through the integration of HP and LP EGR was confirmed, while a proper VNT management allowed for improved fuel consumption level, if an open loop control scheme is followed. At higher engine speed and load, further actions have to be applied to compensate for observed soot emissions increase.

Keywords: diesel engine; exhaust gas recirculation (EGR); low pressure (LP) EGR circuit; proportion of high pressure (HP) and LP EGR; variable nozzle turbine (VNT); pollutant emissions; fuel consumption; NO_X-soot trade-off

1. Introduction

Among the different available technologies to limit NO_X emissions in internal combustion engines (ICEs), exhaust gas recirculation (EGR) has a long and consolidated history, with investigations started about fifty years ago, both on gasoline [1] and diesel engines [2]. Since then, a number of evolution steps were applied to EGR systems, through the fitting of electronic control and exhaust gas cooling, in order to enhance their management while achieving higher effectiveness. In gasoline engines, EGR can also reduce knock occurrence at high load, thus limiting mixture enrichment and improving fuel consumption. In recent years, further developments were considered, starting from the adoption of low pressure (LP) circuit [3,4], as an alternative or coupled to the conventional high pressure (HP) loop [5–7]. Other aspects are related to the integration of EGR circuits with the main engine sub-assemblies, such as fuel injection equipment [8,9] and turbocharging systems [10], either in a single-stage configuration fitted with variable nozzle turbine (VNT) [11] or according to two-stage concepts [12]. Moreover,

other available cleaning options have to be matched to EGR, such as Miller cycle [13] or advanced combustion processes [14,15], extending its use to the whole range of ICEs, such as in marine and stationary applications. Finally, the growing interest in alternative fuels, is leading to further issues to be deepened [16–18].

Current engines are therefore very complex systems, whose performance, fuel consumption, emissions are strongly influenced by each component's behavior and where the number of control variables is continuously increasing. Investigations dealing with the development of suitable management strategies to optimize engine outcomes are therefore mandatory in order to balance and achieve different goals, taking into account the growing worldwide legislation pressure on thermal and chemical emissions.

As broadly discussed in a previous paper [19], most of the available experimental results presented in the literature are focused on large displacement engines [6,20,21]. On the other hand, investigations on dual loop EGR systems were developed mainly through numerical simulations [22–24], limiting test bench activities to model validation. Consequently, little experimental information on the application of hybrid EGR systems in current downsized automotive diesel engines is available. Moreover, as the integration of VNT and EGR systems is approached as in [11], the requirements and problems of control system components and algorithms have increased, or the proper turbocharger matching issues, as in [20]. Therefore, the study presented in this paper aimed at enlarging the knowledge on the reciprocal interactions of turbocharging, HP and LP EGR systems when different control strategies are applied to achieve lower NO_X emissions and fuel consumption. The first goal required the optimization of HP and LP contribution to the overall EGR rate, while the second target demanded the exploitation of the potential offered by the VNT management, thus making experimental planning and results analysis more complex.

Tests were made on a Euro 5 downsized diesel engine (FCA, Turin, Italy), selecting three operating conditions belonging to the engine working area related to the Type Approval cycle. A wide number of engine operating parameters were measured, together with fuel consumption, NO_X and soot emissions.

The influence of dual-loop EGR and turbocharging systems control on intake, exhaust and turbocharger quantities is analyzed and discussed, while showing the prevailing effects of VNT open loop control scheme on fuel consumption, allowing to increase VNT opening, and proving that a larger contribution from the LP loop is requested to reduce NO_X.

2. Experimental Setup

2.1. Engine Test Facility

The experimental campaign was made on an automotive Euro 5 DI diesel engine, fitted on a steady state eddy current dynamometer test bench. Table 1 lists engine main technical characteristics, while Table 2 presents measured parameters, together with the relevant instrumentation. For each instrument, range and accuracy are also shown. Pressure and temperature were acquired in selected sections of the engine intake and exhaust, turbocharging and EGR systems. Moreover, a proper control of coolant, lubricant and charge air temperatures was applied through thermostatic circuits or managing water flow rate to obtain a suitable intercooler efficiency level.

Other measurements were related to the displacement S of the nozzle ring push rod, for which a linear potentiometer was used. Comparing S with its maximum and minimum value (S_{MAX} and S_{MIN}), the VNT opening degree A_{VNT} was evaluated through the equation:

$$A_{VNT} = [(S_{MAX} - S)/(S_{MAX} - S_{MIN})] \times 100\ [\%], \quad (1)$$

ranging from 0% to 100%, when varying the flow area from minimum to maximum.

For low frequency measuring process in steady-state conditions, an automatic data acquisition system was used, including a multichannel scanner, an IEEE bus, a GPIB interface and a personal computer. In-house developed codes in Labview® and Excel® environment allowed to collect and

process data, calculating statistical parameters of measured quantities (average, standard deviation, variation coefficient) and the main engine operating parameters. In-cylinder pressure diagrams were acquired through a dedicated system, sampling different signals at high frequency rates. More details on the measurement equipment used in this study are presented in [19].

Table 1. Characteristics of tested engine. EGR: exhaust gas recirculation; and HP: high pressure.

Engine Type	Four-Stroke, Diesel
Cylinders	4 in-line
Bore (mm) × stroke (mm)	69.9 × 82
Displacement (cm^3)	1248
Compression ratio	16.8:1
Valves for cylinder	4
Maximum power	70 @ 4000 rpm
Maximum torque	200 @ 1500–3000 rpm
Fuel injection system	Direct injection, Multijet II common rail with solenoid injectors, maximum pressure 1650 bar
Turbocharging system	Single stage, variable nozzle turbine, intercooler
EGR system	HP, cooled

Table 2. Measured parameters and instrumentation. FSN: filter smoke number.

Measured Quantity	Instrument	Range	Accuracy
Engine speed	Inductive pick-up	0–5000 rpm	±10 rpm
Engine torque	Eddy current dynamometer	0–250 Nm	±1.25 Nm
Fuel mass flow rate	AVL 733S dynamic measuring equipment	0–37.5 kg/h	0.81% for a measured value of 5 g, 0.42% for 10 g, 0.2% for 25 g
Air mass flow rate	Hot wire air flow meter	0–1000 mg/stroke	±5 mg/stroke
Exhaust smoke	AVL 415 variable sampling smoke meter	0–10 FSN	±0.1 FSN
NO_X concentration	Rosemount 951 CLA analyzer	0–250 ppm	±1.25 ppm
		0–1000 ppm	±5 ppm
Intake and exhaust CO_2 concentration	Beckman 864 NDIR analyzers	0%–2.67%	0.0267%
		0%–16%	0.16%
Turbocharger rotational speed	Eddy current probe	200–400,000 rpm	36 rpm
Temperatures (intake circuit, lubricant, coolant, etc.)	4-wire RTD	0–350 °C	0.15 °C + 0.002 × measured value
Temperatures (exhaust and EGR circuits)	K type TC	0–1200 °C (class 2)	±2.5 °C or
			±0.75% × measured value (class 2)
Pressures	Strain gauge	−1–0.6 bar	<±0.2% × full scale
		0–2.5 bar	
In-cylinder pressure	Kistler 6125B	0–250 bar	<±0.5% × full scale
	Kiag Swiss 5001 charge amplifier		<±1% × full scale
Fuel pressure	Kistler 4067A2000	0–2000 bar	<±0.5% × full scale
	Kistler 4618A2 amplifier		<±0.2% × full scale

2.2. Engine Management System

The engine management system was based on an open electronic control unit (ECU), fitted with an EPROM emulator module (Magneti Marelli, Bologna, Italy), and an ETAS® MAC2F interface connecting the ETK module (ETAS, Stuttgart, Germany) to a dedicated PC. The INCA (ETAS, Stuttgart, Germany) software was used to show engine operating parameters, to select maps stored in the ECU and to change control variables in real time according to the experimental program.

In particular, HP EGR system was managed through a closed loop scheme, comparing the relative air-fuel ratio (AFR) set point with the actual value, given by the measured air mass flow rate and the calculated fuel mass flow rate. The duty-cycle (DC) of the electric HP EGR valve (DC_{EGR}) was then modulated according to the resulting difference, thus adapting its opening degree.

Turbocharger turbine was controlled through open or closed loop strategies, selected by the ECU according to the engine operating condition. The first was applied by setting proper duty-cycle values of an electro-pneumatic valve (DC_{VNT}), thus obtaining fixed values of A_{VNT}. As the resulting pressure level is below the atmospheric pressure, the maximum duty-cycle (DC_{VNT} = 100%) corresponded to the fully closed position (A_{VNT} = 0). The comparison of an intake pressure set point with the measured level allowed to apply the closed loop control scheme, resulting in proper changes of DC_{VNT} to reduce the calculated difference.

2.3. High and Low Pressure Exhaust Gas Recirculation Circuits

Figure 1 shows engine scheme, displaying the standard HP EGR system and the prototype LP EGR circuit, added for the investigations on the integrated control of EGR and turbocharging systems according to a widely adopted solution [20,21]. A selection of engine operating parameters is also presented in the figure, referring to those discussed in Section 3. A diesel oxidation catalyst and particulate filter were not fitted on the engine during the tests, to evaluate the influence of the hybrid EGR system on raw soot emissions, even if compressor rotor and blades were more stressed by particles.

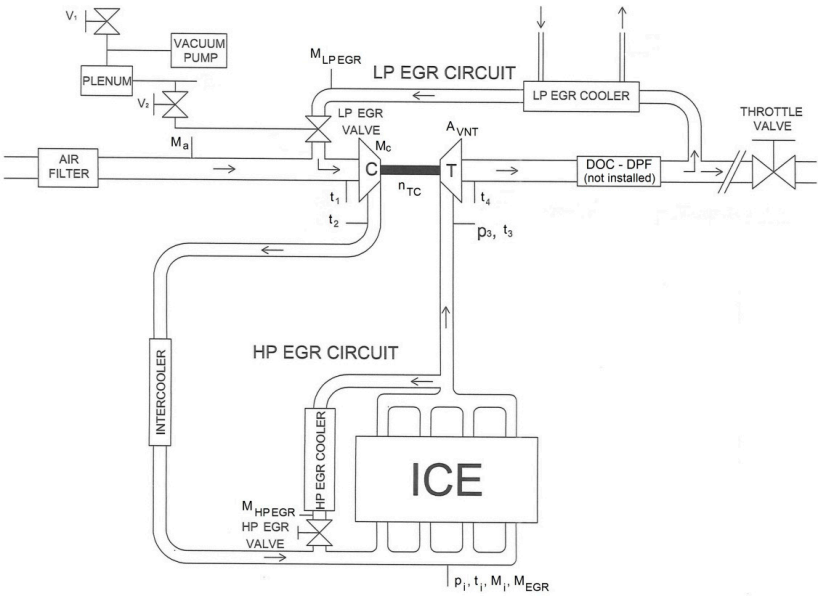

Figure 1. Hybrid EGR system layout. LP: low pressure; VNT: variable nozzle turbine; DOC: diesel oxidation catalyst; DPF: diesel particulate filter; and ICE: internal combustion engine.

On the other hand, engine management and tests development were simplified, due to the absence of the required periodic filter regeneration phases. In order to reproduce suitable pressure levels along the exhaust circuit and in the LP EGR loop, a throttle valve (TV) was fitted at its terminal (Figure 1), whose settings will be analyzed when discussing Table 3. The LP EGR valve was manually controlled through a vacuum signal, while the EGR mass flow rate in the long route loop depended also on the opening position of the above mentioned TV.

EGR rate (f_{EGR}) is expressed as the ratio between recirculated gas and total engine mass flow rate (Equation (2)):

$$f_{EGR} = [M_{EGR}/(M_{EGR} + M_a + M_f)] \times 100\ [\%]. \quad (2)$$

Following a common approach [21,25], f_{EGR} was evaluated through measurements of ambient, intake and exhaust carbon dioxide concentrations, allowing to apply Equation (3):

$$f_{EGR} = [(X_{CO_2\,i} - X_{CO_2\,a})/(X_{CO_2\,e} - X_{CO_2\,a})] \times 100\ [\%]. \quad (3)$$

Estimated levels of M_{EGR} corresponded to the total mass of recirculated gases when both circuits were used or to the mass flowing in the activated circuit when only one was operated. In the first case, the contribution from each loop was calculated through a simplified energy balance between the intake air and the recirculated gases from the two circuits, considering measured temperature levels for each flow, neglecting heat losses and variations of constant pressure specific heat with temperature.

It is well known that one of the consequences of EGR technique application is the reduction of oxygen concentration at the engine intake ($X_{O_{2\,i}}$), representing the dilution effect [1,2,18]. Therefore, the maximum EGR rate, which can be applied without unacceptable penalties in soot emission and in engine performance, depends on AFR corresponding to the requested engine load, being higher at low brake mean effective pressure (*bmep*) values. At the same time, oxygen content in the exhaust/recirculated gases ($X_{O_{2\,e}}$) depends on the same parameter. Useful relationship to link intake and exhaust oxygen concentrations, EGR level and engine load were demonstrated in [25], where a charge dilution index (*CDI*) was also introduced according to Equation (4):

$$CDI = \text{EGR level/Load level} = [(X_{O_{2\,a}} - X_{O_{2\,i}})/(X_{O_{2\,i}} - X_{O_{2\,e}})], \quad (4)$$

to normalize the effect of load on EGR and to allow the comparison of EGR rate in different engine operating conditions [25].

In this investigation, intake and exhaust oxygen concentrations and *CDI* values were estimated according to the measured levels of air and EGR mass flow rates and to the calculation of in-cylinder relative AFR following the relationship presented in [25,26].

Table 3. Schedule of experimental activities. *ID*: identification number; *bmep*: brake mean effective pressure; AFR: air-fuel ratio; TV: throttle valve; and pos.: position.

Operating Condition *ID* = *n* × *bmep* (rpm × bar)	Control Variables (Fixed in Each Test Set)	Control Variables (LP EGR and VNT Control)	Test Sets [2]
No. 1 = 1500 × 2	Relative AFR Exhaust TV position	LP EGR valve opening VNT opening degree	Rel.AFR = 3.01 − TV pos. 1
			Rel.AFR = **2.90** [1] − TV pos. **1** [1]/2/3
			Rel.AFR = 2.77 − TV pos. 1/2
			Rel.AFR = 2.62 −TV pos. 1/2
No. 2 = 2000 × 5	Relative AFR Exhaust TV position	LP EGR valve opening VNT opening degree	Rel.AFR = 1.94 − TV pos. 1
			Rel.AFR = **1.80** [1] − TV pos. **1**/2/3
			Rel.AFR = 1.67 − TV pos. 1/2
No. 3 = 2500 × 8	Relative AFR	LP EGR valve opening	Rel.AFR = 1.60 − Intake pressure = 1.48 bar − TV pos. 1
	Exhaust TV position		Rel.AFR = **1.60** [1] − Intake pressure = **1.52** [1]/1.57 bar − TV pos. 0/**1** [1]
	Intake pressure		Rel.AFR = 1.47 − Intake pressure = 1.52 bar − TV pos. 1

[1] Standard/reference values shown in bold; [2] Constant operating parameters (ECU standard calibration levels): pilot, pre and main start of injection. Pilot and pre injected quantity. Rail pressure.

2.4. Testing Procedure

Selection of engine operating conditions was referred to low and medium levels of *bmep* and rotational speed *n*, as they are prevailing when dealing with type approval and real world operations in the automotive field. Moreover, different interactions between EGR and turbocharging systems were outlined in these conditions, allowing to analyze a wide range of relationship between the engine operating quantities. The first column of Table 3 presents the identification number of each selected working point, together with the relevant values of *n* and *bmep*. Considering the mass and gearbox ratios of cars belonging to the B and C-segment equipped with the tested engine, conditions can be referred to the new European driving cycle (NEDC). In particular, points No. 1 and 2 represent the

average operations related to speed levels between 30 and 90 km/h, while point No. 3 is related to the extra-urban acceleration from 100 to 120 km/h.

Tests aimed at the assessment of the potential in NO_X reduction resulting from the application of a LP EGR system, used either simultaneously with the standard short route circuit or as a stand-alone option. To compensate the negative influence of long route loop on fuel consumption, VNT control was added in order to reduce engine pressure gradient and pumping losses.

To achieve these objectives, four different control variables were considered in all the working points. In operating conditions No. 1 and 2, each set of test was defined according to a fixed value of relative AFR and to the position of the throttle valve at the end of the exhaust circuit. For every experimental set, the HP EGR circuit was used in the first operating mode. Then, LP EGR loop was activated, gradually increasing the relevant valve opening degree. In these modes, A_{VNT} was maintained at its standard value by fixing the corresponding duty-cycle in the ECU map. At the maximum LP EGR valve opening level, the VNT control was added, increasing A_{VNT}.

In operating condition No. 3, turbine was controlled by the ECU according to the closed loop scheme based on the intake pressure set point. Therefore, experimental sets were identified through fixed levels of three control variables (i.e., relative AFR, exhaust TV position and intake pressure). The first mode was again related to recirculation from the short route loop only, while a growing contribution from the LP circuit was then added by managing the relevant valve.

Table 3 summarizes the schedule of the experimental campaign, showing selected values of relative AFR, valve settings for exhaust throttle and, for condition No. 3, intake pressure. In the first case, standard levels stored in the ECU represented the reference condition when exhaust gas were recirculated only through the HP circuit. As regards the different settings of the exhaust throttle valve, position 1 corresponded to the pressure level at the turbine exit when a regenerated diesel particulate filter (DPF) was considered. More closed settings were actuated in positions 2 and 3, leading to an increase in recirculated gases from long route loop, while position 0 corresponded to a more opened setting.

3. Results and Discussion

Results are presented and discussed in this section considering selected parameters, which outline the most significant interactions between EGR and turbocharging systems. Graphs are built as a function of LP proportion, which is the ratio between LP and total mass flow rates of recirculated gases. Based on the definition of each test set, the analysis of every curves has to be made starting from the left hand side (M_{LPEGR}/M_{EGR} = 0, HP EGR loop activated). Moving towards the right side, contribution from the LP loop grows, until the HP EGR circuit is deactivated (M_{LPEGR}/M_{EGR} = 1). To obtain this operating mode, suitable A_{VNT} control was applied in points No. 1 and 2 [19], while just increasing LP contribution in point No. 3 forced the ECU to close the HP EGR valve. In this testing condition, it was also possible to obtain different modes characterized by the null level of HP proportion, by changing A_{VNT} value until a threshold limit of exhaust smoke (i.e., 3 FSN) was reached.

Each graph shows results for selected sets of the three operating conditions, in order to highlight differences in observed trends. For points No. 1 and 2, continuous lines are associated to standard levels of VNT opening degree, while dotted lines are referred to A_{VNT} control with increased values. In each figure, reference values are shown, corresponding to observed levels when applying the standard HP EGR setting fixed by the engine manufacturer.

Discussion is developed considering the behavior of engine quantities referred to the intake circuit (Section 3.1), EGR circuits (Section 3.2), turbocharger (Section 3.3) and exhaust circuit (Section 3.4). Finally, trade-offs between fuel consumption, NO_X and soot emissions are analyzed (Section 3.5).

3.1. Intake Circuit

Levels of compressor mass flow rate M_c are shown in Figure 2. This quantity is given by the sum of air and LP EGR rate mass flow rates. Taking into account that the first parameter (not shown) is

constant in operating conditions No. 1 and 2 for the standard level of A_{VNT}, while presented slight reduction in point No. 3, trends show the increasing contribution from the LP circuit when opening the relevant valve. Variations are apparent when changing relative AFR (in particular for operating modes with HP EGR only). When higher values of A_{VNT} were applied in points No. 1 and 2, reductions of both contributions were observed. Due to the different VNT control in 2500 × 8 condition, a rising trend is observed in the whole range of LP proportion.

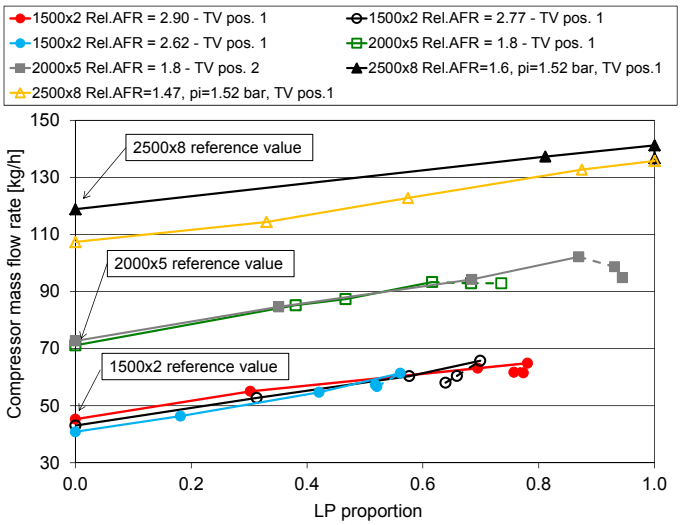

Figure 2. Compressor mass flow rate as a function of LP proportion in different operating modes.

Figure 3 presents the behavior of intake mass flow rate M_i, given by the sum of air and recirculated gases from both the EGR loops. This parameter can also be evaluated as the sum of compressor and HP EGR mass flow rates. Changes between points No. 1 and 2 on one hand and point No. 3 on the other are shown, always due to the alternative VNT control schemes. In the first case, the increase proves that LP EGR overcomes the reduction in HP EGR for constant A_{VNT} values, while in the second, observed levels are almost constant, as variations in contribution from the two EGR circuits are balanced.

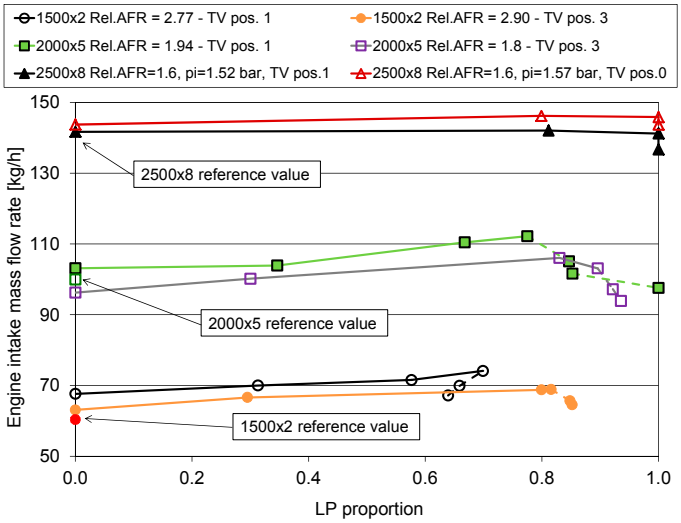

Figure 3. Engine intake mass flow rate as a function of LP proportion in different operating modes.

Opening the VNT leads to a reduction in intake mass flow rates, but with different effects to LP proportion, which may decrease (one set of point No. 1), increase (second set of point No. 1, all

sets of point No. 2) or remain at level = 1.0 (point No. 3). Measured values of intake pressure p_i are displayed in Figure 4. The constant trend in 2500 × 8 condition is obviously due to the VNT closed loop control scheme. In points No. 1 and 2, the activation of LP loop and the growth of its contribution leads to an increase in this quantity, outlining one of the effects of the different interaction between this circuit and the turbocharging system, which is more remarkable at intermediate level of *n* and *bmep*. When controlling VNT opening degree, a significant reduction in p_i is obviously observed, with final levels going below the reference values for the adopted A_{VNT} settings.

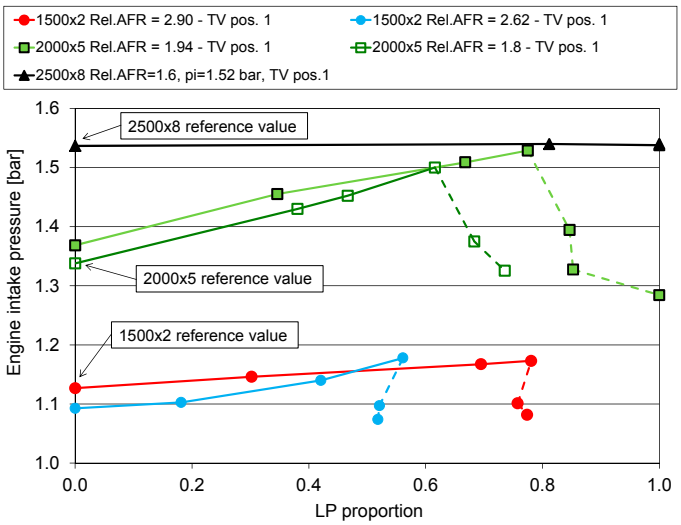

Figure 4. Engine intake pressure as a function of LP proportion in different operating modes.

Values of compressor exit temperature T_2 are presented in Figure 5. Major variations are observed for experimental points No. 1 and 2, as compressor exit temperature is influenced by the rise in compressor inlet temperature T_1 (as a consequence of LP EGR activation and ranging between 5 and 20 °C) and p_i.

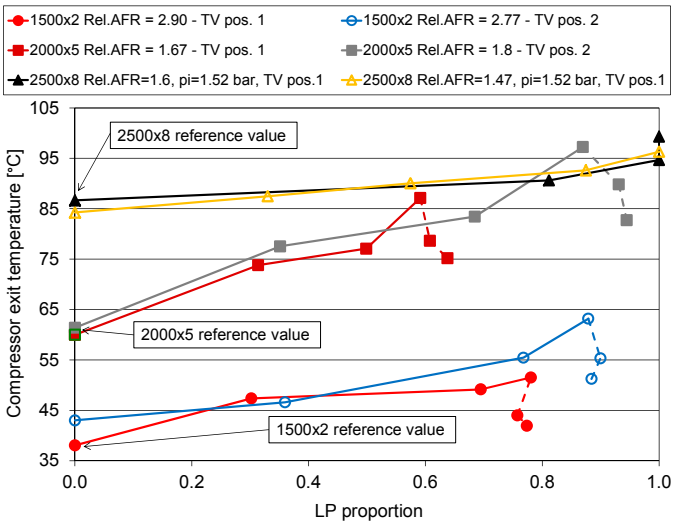

Figure 5. Compressor exit temperature as a function of LP proportion in different operating modes.

When opening A_{VNT}, the strong decrease in intake pressure overcame the influence of T_1, leading to reduced T_2 levels. In point No. 3, as boost pressure is kept constant, only the temperature increase at the compressor inlet influenced T_2, resulting in a lower growth.

Following the engine intake circuit (Figure 1), after the compressor two main components affects charge flow, modifying mass rate, pressure and temperature, i.e., the intercooler and the HP EGR valve. Values of intake temperature are depicted in Figure 6, showing the beneficial influence of LP EGR [7]. When its contribution increased (in particular up to a level around 70%), a significant reduction in t_i was observed, due to the cooling effect of intercooler on this share of recirculated gas.

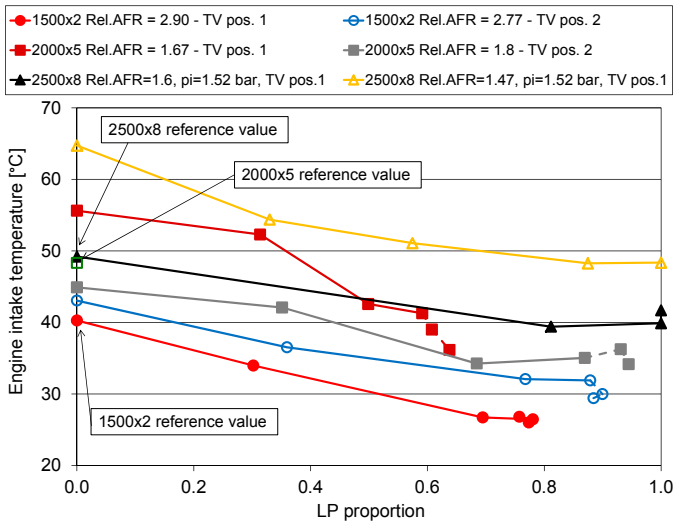

Figure 6. Engine intake temperature as a function of LP proportion in different operating modes.

3.2. Exhaust Gas Recirculation Circuits

Analysis of the EGR circuits' behavior is a fundamental aspect of the investigation, as they influence engine and turbocharger performance, aside from determining emission levels. Considering the overall operation of the two loops, trends of total EGR mass flow rate are presented in Figure 7. Increasing levels are apparent when adding LP contribution, with similar slope in the different operating conditions, with a few exception (especially for the 2000 × 5 point when applying a high HP EGR rate). When opening VNT, observed values show significant differences according to the experimental points, as M_{EGR} remained quite constant in 1500 × 2, while reducing in 2000 × 5, due to the prevailing effect of HP EGR decrease. For 2500 × 8, the whole curve corresponded to an increase in A_{VNT}, leading M_{LPEGR} and M_{EGR} to rise, while M_{HPEGR} reduced up to its complete exclusion.

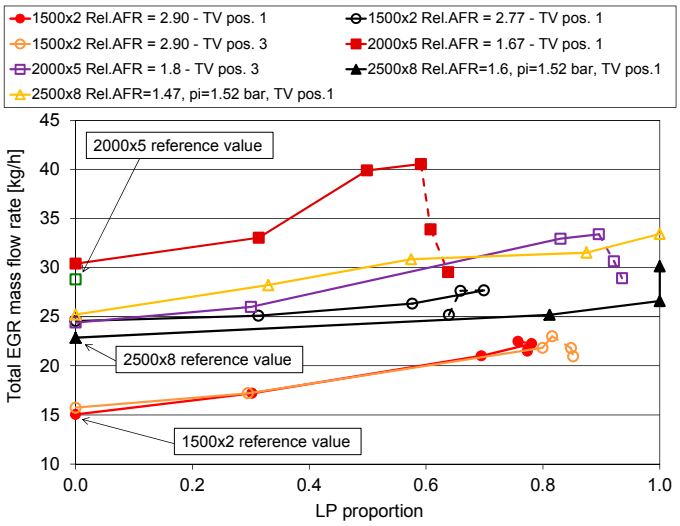

Figure 7. Total EGR mass flow rate as a function of LP proportion in different operating modes.

Non-dimensional parameters are usually adopted to evaluate EGR levels, comparing it to intake charge through the EGR rate. As previously stated (Section 2.3), a Charge Dilution Index was recently introduced in [25], to normalize the effect of load on EGR while comparing EGR rate in different engine operating conditions. The relationship between EGR rate and *CDI* is presented in Figure 8, identifying observed/calculated values according to the experimental points.

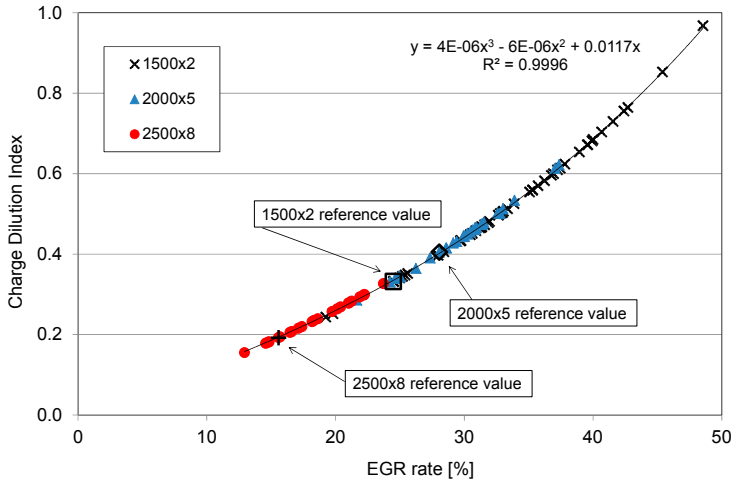

Figure 8. Relationship between EGR rate and charge dilution index in tested operating modes.

Notwithstanding *CDI* was obtained through the estimation of intake and exhaust oxygen concentrations, a good correlation with EGR rate is shown, which is in line with trend presented in [25]. Therefore, this parameter will be further investigated, taking into account its potential to develop general correlation with combustion parameters derived by in-cylinder pressure diagrams processing (pressure derivative and rate of heat release) for modeling purposes.

On the other hand, an extended range for the two parameters is apparent for 1500 × 2, progressively reduced when considering condition No. 2 (2000 × 5) and No. 3 (2500 × 8), as it could be anticipated by the corresponding levels of engine load and relative AFR. Reference values are always at the lower hand side of the intervals, confirming the significant increase in EGR rate allowed by the prototype LP circuit. Taking into account this outcome, it can be concluded that the prototype LP loop present a satisfactory sizing, balancing the request of recirculated flow rate in the low-medium range of engine speed and load and reproducing proper levels of pressure losses in the circuit.

3.3. Turbocharger

Turbocharging systems are key elements to define engine performance and operations, while their control is a fundamental aspect to achieve satisfactory levels of fuel consumption and emissions, while obtaining acceptable engine transient response.

Being strictly related, the first two parameters discussed in this section are engine pressure gradient, whose behavior is represented in Figure 9, and VNT opening degree, shown in Figure 10.

Engine pressure gradient has probably the strongest relations with all the involved sub-systems and components, interacting with HP EGR mass flow rate, engine pumping losses and fuel consumption, compressor and turbine operating points and nozzle turbine control strategies.

At constant A_{VNT} level and when only HP EGR loop is activated (LP proportion = 0), its value depended on HP EGR valve opening, that is, on relative AFR level. Introducing and increasing LP EGR contribution, observed trends depended on VNT control scheme. In open loop (i.e., in points No. 1 and 2), a significant increase of pressure gradient was apparent when rising LP proportion, until the VNT opening compensate for this effect (dotted lines in Figures 9 and 10), leading its values below the reference ones, with positive influence on fuel consumption.

In closed loop (condition No. 3), ECU opened nozzle turbine (Figure 10) when LP EGR circuit was activated, in order to keep the intake pressure at set point level, compensating for its contribution to compressor mass flow rate and modifying compressor working point. Consequently, A_{VNT} shows an increasing trend (Figure 10), leading to slight decrease of exhaust pressure (i.e., turbine inlet pressure).

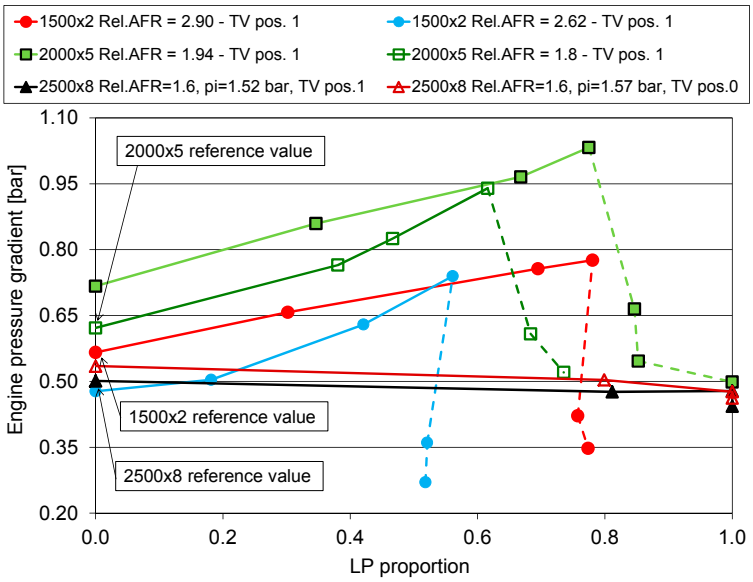

Figure 9. Engine pressure gradient as a function of LP proportion in different operating modes.

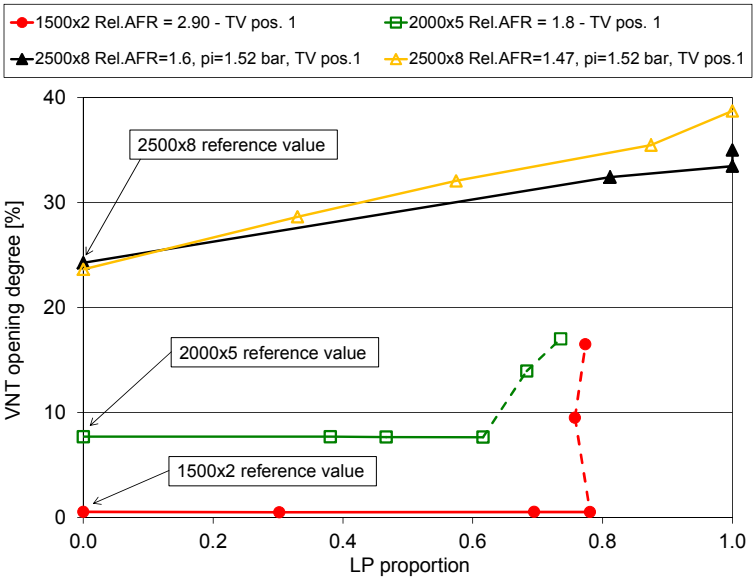

Figure 10. VNT opening degree as a function of LP proportion in different operating modes.

Measured levels of turbocharger rotational speed n_{TC} are presented in Figure 11. Trends confirm the influence of LP EGR contribution and A_{VNT} control in operating points No. 1 and 2. It is interesting to note that levels attained at higher VNT settings are anyway higher than the reference ones, which should help in transient operations starting from these part load conditions. In point No. 3, increase of turbine mass flow rate (which differs from compressor one, Figure 2, only for fuel mass flow rate) overcame VNT opening at reduced values of HP proportion, resulting in a slight rise in turbocharger speed.

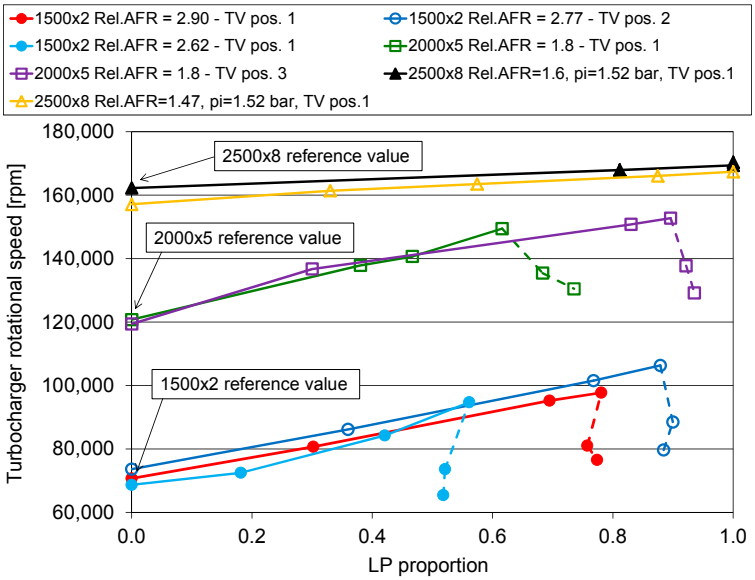

Figure 11. Turbocharger rotational speed as a function of LP proportion in different operating modes.

3.4. Exhaust Circuit

Trends of turbine inlet pressure p_3 are shown in Figure 12. In points No. 1 and 2, again LP EGR effect and A_{VNT} control play a major role in determining the observed behavior. In point No. 3, VNT control, jointly with the almost constant trends in M_i, led to a slight reduction in p_3.

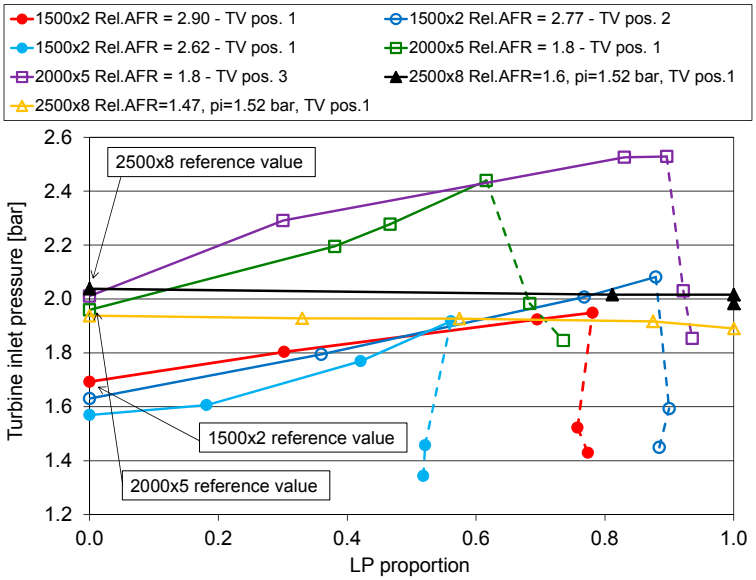

Figure 12. Turbine inlet pressure as a function of LP proportion in different operating modes.

Temperature levels at turbine inlet and exit (T_3 and T_4) show minor variations in the different operating modes. As an example, values at the turbine exit are presented in Figure 13, showing slight reductions in points No. 2 and 3 when increasing LP contribution and a different influence of VNT opening in conditions 1 and 2. Taking into account the position of the DPF, it can be concluded that DPF regeneration would not be significantly affected by the integrated control of EGR and turbocharging systems.

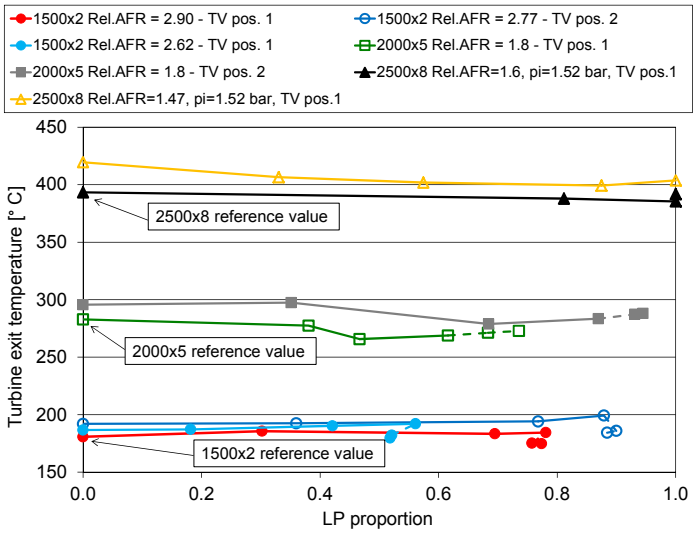

Figure 13. Turbine exit temperature as a function of LP proportion in different operating modes.

3.5. Fuel Consumption and Emissions Trade-Off

In the previous sections, an extended analysis of the influence of control strategies for both the EGR circuits and the turbocharger on engine operating parameters was developed, in order to outline the potential of LP EGR circuit fitted to a state-of-the-art diesel engine while showing the strong interactions with controlled systems.

As energy consumption and pollution issues are the main driving forces of engine development, it is mandatory to conclude the results discussion summarizing the main achievements in these fields, reporting the main important trade-offs between brake specific fuel consumption (bsfc), NO_X emission ($bsNO_X$) and soot emission (bsS).

Figure 14 shown a selection of these curves for fuel consumption and nitrogen oxides emission, confirming the different behavior of some engine quantities in the tested operating conditions.

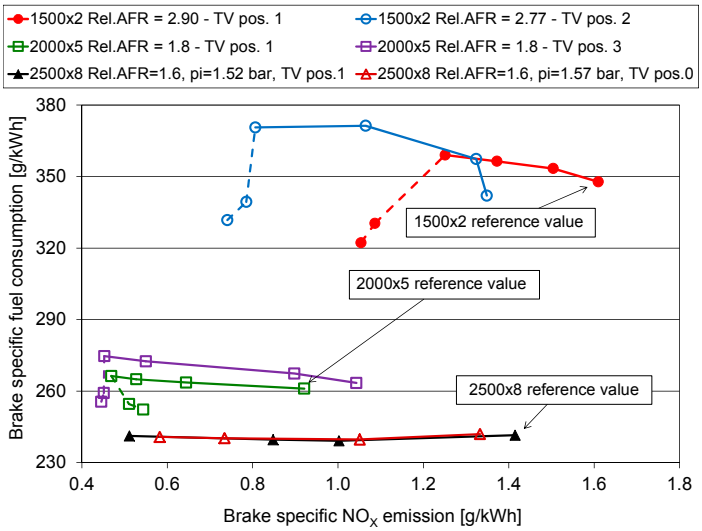

Figure 14. Trade-off between brake specific NO_X emissions and fuel consumption in different operating modes.

Considering the reference values shown in Figure 14 (Euro 5 settings), significant reduction were achieved for $bsNO_X$, ranging between −51% (point No. 2) and −64% (point No. 3), that is, around

the requested improvement from Euro 5 to Euro 6 limits. Table 4 lists the corresponding values for controlled parameters: it is interesting to note the prevailing effect of LP contribution to NO_X decrease in the three tested points to achieve the mentioned variations. It has also to be outlined that proposed strategies are referred to steady state operating conditions, as the available test bench doesn't allow to perform dynamic tests. In real world operations, transient corrections will probably be requested [27,28], to take into account different time delays of high and LP EGR circuits, mainly related to their length.

Table 4. Optimal control strategies for NO_X and fuel consumption reduction in tested steady state operating conditions.

Operating Condition *ID* = *n* × *bmep* (rpm × bar)	Relative AFR	Exhaust TV Position	VNT Opening Degree (%)	LP Proportion
No. 1 = 1500 × 2	2.77	2	17.7	0.884
No. 2 = 2000 × 5	1.8	3	17.3	0.935
No. 3 = 2500 × 8	1.6	1	35 (1.52 bar [1])	1.0

[1] Intake pressure set-point.

Referring to fuel consumption, a significant decrease can be observed in the corresponding modes of operating conditions 1 (−4.6%) and 2 (even if at a lower extent, −2.1%), obtained with A_{VNT} levels around 17% (Table 4), i.e., higher than the reference ones (Figure 10). In the third condition, no variations were attained due to the different VNT control.

The comparison of bsfc trends with those presented in Figure 9 for engine pressure gradient confirms the strict relationship between these parameters, outlining the prevailing effect of pumping losses over every variations on combustion development induced by EGR activation and control.

Soot and NO_X emissions trade-off is presented in Figure 15. In this case, penalties in soot are probably acceptable in point No. 1 (+23.3%, referring to the mode with the best NO_X reduction) and No. 2 (+48.4%), while in condition No. 3 bsS is more than doubled, requiring further actions to limit this increase, such as a change in fuel injection pressure. The different order of magnitude of measured bsS variations are related to relative AFR levels (Table 3).

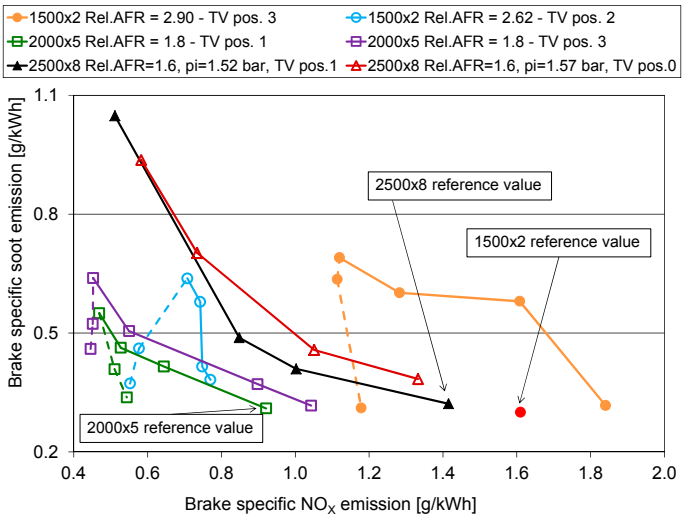

Figure 15. Trade-off between brake specific NO_X and soot emissions in different operating modes.

From a more general point of view, observed trends confirm that it is possible to move trade-off curves towards lower values, while modifying their trend through VNT control. In operating condition No. 3, a more conventional behavior is apparent, while control variables (in particular, engine intake pressure) have to be varied in a more significant way in order to modify the position of trade-off curves.

Trends of NO_X and soot emissions can be related to measurement and processing of in-cylinder pressure diagrams, referring their values to maximum pressure and heat release, respectively.

Figure 16 shows bsNO_X values as a function of maximum in-cylinder pressure. In points No. 1 and 2, observed complex behavior is related to EGR fraction and VNT opening degree, influencing intake pressure and mass flow rate and the development of combustion process. In point No. 3, a more expected trend is apparent, with NO_X reduction corresponding to lower levels of p_{MAX} for each set.

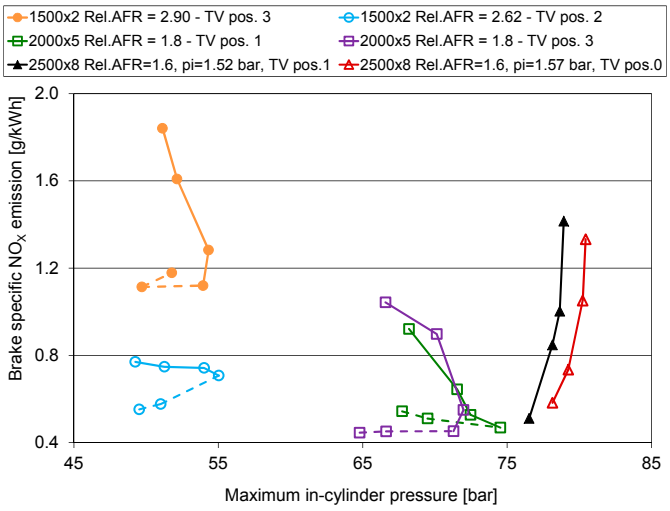

Figure 16. Relationship between maximum in-cylinder pressure and brake specific NO_X emissions in different operating modes.

Figure 17 presents bsS values as a function of heat released in premixed mode of combustion referred to the main injection, calculated from heat release curves as defined in [29]. It is well known [30], that a lower soot emission is associated to a more intense premixed combustion. Therefore, an inverse relationship is expected between these parameters, as shown in [29] and is apparent in Figure 17 for one test set for each working point. Moreover, the same correlation was verified for all the operating modes of point No. 3, allowing to assess the linear link for a wider range of soot emissions and premixed heat release values, as proved by the high level of determination coefficient.

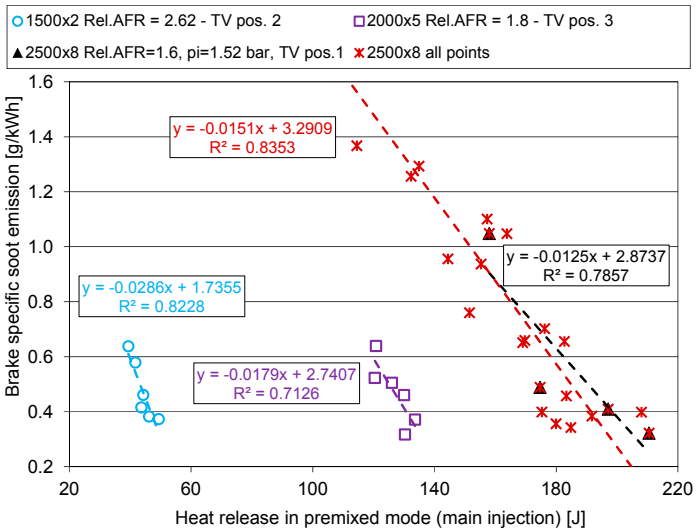

Figure 17. Relationship between heat released in premixed mode and brake specific soot emissions in different operating modes.

4. Conclusions

The experimental study on the development of integrated control strategies of turbocharging and high and LP EGR systems in an automotive diesel engine allowed us to study in depth different aspects referring to the reciprocal interactions between the different subsystems and to the influence on engine behavior. Among the achieved outcomes, some major points can be summarized:

- Results are strongly influenced by the applied VNT management scheme: among the selected operating conditions, open loop control is applied at low levels of speed and *bmep* (i.e., in 1500 × 2 and 2000 × 5 test point), while boost pressure is closed loop controlled when increasing these parameters (i.e., in 2500 × 8 condition).
- When activating and increasing LP EGR contribution, intake and exhaust parameters (mass flow rate, temperature and pressure levels) are significantly modified. In particular, the increase of engine pressure gradient and compressor/intake mass flow rate leads engine and turbocharger to work in conditions similar to those without EGR.
- With VNT open loop control, fuel consumption is strongly influenced by engine pressure gradient, representing an approximate index of pumping losses. Applying proper settings of VNT position, significant benefit can be achieved for this quantity (−4.6% and −2.1% in operating condition No. 1 and 2, respectively).
- Referring to the standard engine behavior (levels measured in Euro 5 configuration), reduction between 51% and 64% for NO_X emission was obtained, through the increase of EGR rate and a prevailing (points No. 1 and 2) or complete (point No. 3) contribution from LP loop. As a consequence, soot emission was increased, but while a reasonable rise was observed in points No. 1 and 2 (with significant benefits obtained through VNT opening), excessive penalties affected point No. 3, therefore requiring the adoption of further measures to compensate for this negative aspect.
- EGR technique can be enhanced through the integration of HP and LP circuits. As the second option has different interactions with turbocharger compressor and turbine, a wide potential is offered by the integrated control of these systems, not only to improve fuel consumption and NO_X emissions, but also to help engine in transient conditions.

Author Contributions: Giorgio Zamboni and Massimo Capobianco conceived and designed the experiments; Giorgio Zamboni and Simone Moggia performed the experiments and processed data; Giorgio Zamboni and Massimo Capobianco analyzed the data; Giorgio Zamboni wrote the paper.

Conflicts of Interest: The authors declare no conflict of interest.

Abbreviations

bmep	Brake mean effective pressure
bsfc	Brake specific fuel consumption
$bsNO_X$	Brake specific nitrogen oxides emission
bsS	Brake specific soot emission
f	Mass flow fraction
n	Rotational speed
p	Pressure
T	Temperature (°C)
A	Opening degree
AFR	Air-fuel ratio
CDI	Charge dilution index
DC	Duty-cycle
DI	Direct injection
ECU	Electronic control unit
EGR	Exhaust gas recirculation
FSN	Filter smoke number
HP	High pressure
LP	Low pressure

M	Mass flow rate
NEDC	New European Driving Cycle
S	Nozzle ring push rod displacement
TV	Throttle valve
VNT	Variable nozzle turbine
X	Volumetric concentration

Subscripts

a	Air
c	Compressor
f	Fuel
i	Intake
e	Exhaust
CO_2	Carbon dioxide
EGR	Exhaust gas recirculation
HP	High pressure
LP	Low pressure
MAX	Maximum
MIN	Minimum
O_2	Oxygen
VNT	Variable nozzle turbine
TC	Turbocharger
1	Compressor inlet
2	Compressor exit
3	Turbine inlet
4	Turbine exit

References

1. Quader, A.A. Why intake charge dilution decreases nitric oxide emission from spark ignition engines. *SAE Int.* **1971**. [CrossRef]
2. Plee, S.L.; Ahmad, T.; Myers, J.P. Flame temperature correlation for the effects of exhaust gas recirculation on diesel particulate and NO_X emissions. *SAE Int.* **1981**. [CrossRef]
3. Lundqvist, U.; Smedler, G.; Stalhammar, P. A comparison between different EGR systems for HD diesel engines and their effect on performance, fuel consumption and emissions. *SAE Int.* **2000**. [CrossRef]
4. Ivaldi, D.; Lisbona, M.G.; Tonetti, M. An improved EGR system concept for diesel engines towards fuel neutral emissions. *Int. J. Veh. Des.* **2006**, *41*, 307–325. [CrossRef]
5. Zamboni, G.; Capobianco, M. Experimental study on the effects of HP and LP EGR in an automotive turbocharged diesel engine. *Appl. Energy* **2012**, *94*, 117–128. [CrossRef]
6. Mao, B.; Yao, M.; Zheng, Z.; Li, Y.; Liu, H.; Yan, B. Effects of dual loop EGR on performance and emissions of a diesel engine. *SAE Int.* **2015**. [CrossRef]
7. Park, J.; Choi, J. Optimization of dual-loop exhaust gas recirculation splitting for a light-duty diesel engine with model-based control. *Appl. Energy* **2016**, *181*, 268–277. [CrossRef]
8. Meloni, R.; Naso, V. An insight into the effect of advanced injection strategies on pollutant emissions of a heavy-duty diesel engine. *Energies* **2013**, *6*, 4331–4351. [CrossRef]
9. Ge, J.C.; Kim, M.S.; Yoon, S.K.; Choi, N.J. Effects of pilot injection timing and EGR on combustion, performance and exhaust emissions in a common rail diesel engine fueled with a canola oil biodiesel-diesel blend. *Energies* **2015**, *8*, 7312–7325. [CrossRef]
10. Dong, T.; Zhang, F.; Liu, B.; An, X. Model-based state feedback controller design for a turbocharged diesel engine with an EGR system. *Energies* **2015**, *8*, 5018–5039. [CrossRef]
11. Shutty, J. Control strategy optimization for hybrid EGR engines. *SAE Int.* **2009**. [CrossRef]
12. Albin, T.; Ritter, D.; Liberda, N.; Abel, D. Boost pressure control strategy to account for transient behavior and pumping losses in a two-stage turbocharged air path concept. *Energies* **2016**, *9*. [CrossRef]
13. He, S.; Du, B.G.; Feng, L.Y.; Fu, Y.; Cui, J.C.; Long, W.Q. A numerical study on combustion and emission characteristics of a medium-speed diesel engine using in-cylinder cleaning technologies. *Energies* **2015**, *8*, 4118–4137. [CrossRef]
14. Lee, Y.; Huh, K.Y. Analysis of different modes of low temperature combustion by ultra-high EGR and modulated kinetics in a heavy duty diesel engine. *Appl. Therm. Eng.* **2014**, *70*, 776–787. [CrossRef]

15. Jung, D.; Iida, N. Closed-loop control of HCCI combustion for DME using external EGR and rebreathed EGR to reduce pressure-rise rate with combustion-phasing retard. *Appl. Energy* **2015**, *138*, 315–330. [CrossRef]
16. Yoon, S.H.; Han, S.C.; Lee, C.S. Effects of high EGR rate on dimethyl ether (DME) combustion and pollutant emission characteristics in a direct injection diesel engine. *Energies* **2013**, *6*, 5157–5167. [CrossRef]
17. Solaimuthu, C.; Ganesan, V.; Senthilkumar, D.; Ramasamy, K.K. Emission reductions studies of a biodiesel engine using EGR and SCR for agriculture operations in developing countries. *Appl. Energy* **2015**, *138*, 91–98. [CrossRef]
18. Thangaraja, J.; Kannan, C. Effect of exhaust gas recirculation on advanced diesel combustion and alternate fuels—A review. *Appl. Energy* **2016**, *180*, 169–184. [CrossRef]
19. Zamboni, G.; Moggia, S.; Capobianco, M. Hybrid EGR and turbocharging systems control for low NO_X and fuel consumption in an automotive diesel engine. *Appl. Energy* **2016**, *165*, 839–848. [CrossRef]
20. Suresh, A.; Langenderfer, D.; Arnett, C.; Ruth, M. Thermodynamic systems for Tier 2 Bin 2 diesel engines. *SAE Int. J. Engines* **2013**, *6*. [CrossRef]
21. Park, Y.; Bae, C. Experimental study on the effects of high/low pressure EGR proportion in a passenger car diesel engine. *Appl. Energy* **2014**, *133*, 308–316. [CrossRef]
22. Zeng, X.; Wang, J. A physics-based time-varying transport delay oxygen concentration model for dual-loop exhaust gas recirculation (EGR) engine air-paths. *Appl. Energy* **2014**, *125*, 300–307. [CrossRef]
23. Cornolti, L.; Onorati, A.; Cerri, T.; Montenegro, G.; Piscaglia, F. 1D simulation of a turbocharged diesel engine with comparison of short and long EGR route solutions. *Appl. Energy* **2013**, *111*, 1–15. [CrossRef]
24. Park, J.; Song, S.; Lee, K.S. Numerical investigation of a dual-loop EGR split strategy using a split index and multi-objective Pareto optimization. *Appl. Energy* **2015**, *142*, 21–32. [CrossRef]
25. Asad, U.; Tjong, J.; Zheng, M. Exhaust gas recirculation—Zero dimensional modelling and characterization for transient diesel combustion control. *Energy Convers. Manag.* **2014**, *86*, 309–324. [CrossRef]
26. Asad, U.; Zheng, M. Exhaust gas recirculation for advanced diesel combustion cycles. *Appl. Energy* **2014**, *123*, 242–252. [CrossRef]
27. Millo, F.; Ferrero Giacominetto, P.; Gianoglio Bernardi, M. Analysis of different exhaust gas recirculation architectures for passenger car diesel engines. *Appl. Energy* **2012**, *98*, 79–91. [CrossRef]
28. Luján, J.M.; Guardiola, C.; Pla, B.; Reig, A. Switching strategy between HP (high pressure)-and LPEGR (low pressure exhaust gas recirculation) systems for reduced fuel consumption and emissions. *Energy* **2015**, *90–2*, 1790–1798. [CrossRef]
29. Badami, M.; Mallamo, F.; Millo, F.; Rossi, E.E. Experimental investigation on the effect of multiple injection strategies on emissions, noise and brake specific fuel consumption of an automotive direct injection common-rail diesel engine. *Int. J. Engine Res.* **2003**, *4*, 299–314. [CrossRef]
30. Eastwood, P. *Particulate Emissions from Vehicles*; John Wiley & Sons Ltd.: Chichester, UK, 2008.